JOURNAL OF SOLID STATE CHEMISTRY 41, 221–226 (1982)

Intergrowth of Hexagonal Tungsten Bronze and Perovskite-Like Structures: The Oxides $ACu_3M_7O_{21}$ (A = K, Rb, Cs, Tl; M = Nb, Ta)

A. BENMOUSSA, D. GROULT, F. STUDER, AND B. RAVEAU

Laboratoire de Cristallographie, Chimie et Physique du Solide L.A. 251, I.S.M.R.A., Université de Caen, 14032 Caen Cedex, France

Received July 21, 1981; in final form October 19, 1981

Seven oxides $ACu_3M_7O_{21}$ have been isolated with A = K, Rb, Tl, Cs for M = Ta and A = K, Rb, Cs for M = Nb. These phases are orthorhombic: $a \simeq 28$ Å, $b \simeq 7.50$ Å, and $c \simeq 7.55$ Å, probable space group *Cmmm*. Their structure has been established from an X-ray diffraction study and from high-resolution microscopy observations. The structure consists of an intergrowth of single hexagonal tungsten bronze AM_3O_9 slices and double distorted perovskite $Cu_3M_4O_{12}$ slabs (M = Nb, Ta) in which copper has a square coordination. The host lattice of these compounds can be considered as the member "$n = 1$; $n' = 2$" of a series of intergrowths corresponding to the formulation $|M_3O_9|_n^H\,|M_2O_6|_{n'}^P$.

Introduction

It has been previously shown that the ReO_3 type structure can accommodate the hexagonal tungsten bronze framework. It is indeed the case of the potassium, rubidium and cesium tungsten bronzes (ITB) described by Hussain and Kihlborg (*1*, *2*). The formation of the intergrowth requires a drastic distortion of the ReO_3 network involving a change of the O–Ô–O angles between two neighboring octahedra from 90 to 120° (or 60°) and a tilting of these octahedra around the axis normal to the intergrowth direction. Such a distortion of the perovskite framework can, in fact, be stabilized by insertion of divalent copper or trivalent manganese, owing to the Jahn–Teller effect ensured by these ions as is shown for several ternary manganese oxides (*3*, *4*) and copper oxides (*5–7*) in which all the initial perovskite sites are occupied. The studies of the titanotantalate $Cu_3Ti_2Ta_2O_{12}$ (*8*, *9*) and of the tantalate $CuTa_2O_6$ (*10*) have shown that the occupation of all the perovskite sites is not absolutely necessary to stabilize such a distortion. Moreover the parameter of the pseudocubic cell of $CuTa_2O_6$, very close to that of the hexagonal tungsten bronze (HTB) $KTa_{3.4}O_9$ (*11*) or $TlTa_{3.4}O_9$ (*12*), is favorable to the connection of these two structures. The systems CuM_2O_6–AM_3O_9 (M = Nb, Ta; A = K, Rb, Cs, Tl) were thus investigated. We describe here a series of niobates and tantalates $ACu_3M_7O_{21}$ corresponding to such an intergrowth.

Experimental Methods

Synthesis

All the alkali compounds were prepared in air, in a platinum crucible, from mixtures of A_2CO_3 (A = K, Rb, Cs), CuO, and M_2O_5 oxides (M = Nb, Ta) in ratios corresponding to the final product $ACu_3M_7O_{21}$. The

0022-4596/82/020221-06$02.00/0

thallium oxide was prepared from Tl_2CO_3 under argon. The mixtures were first heated at 800°C in order to decompose the carbonates. The products were then ground and heated at 900 and 1000°C during 24 hr. After each thermal treatment the quenched materials were examined by X-ray powder diffraction using a Guinier camera.

Analysis

The final compounds were characterized by their X-ray diffractograms, using a Philips goniometer for the Cu$K\alpha$ radiation. Owing to their transparency in the electron beam, the niobates could be studied by electron microscopy with a JEOL 120 CX microscope supplied with a goniometer stage (line resolution ≈ 2 Å) or a standard high resolution (line resolution ≈ 1.4 Å). For this study, the powder samples, ground in an agate mortar and dispersed in an ethylic alcohol solution, were then deposited on a carbon-coated grid.

Results

According to the methods previously described, seven isotypic compounds have been synthesized: four tantalates $ACu_3Ta_7O_{21}$ (A = K, Rb, Cs, Tl) and three niobates $ACu_3Nb_7O_{21}$ (A = K, Rb, Cs). Although the thallium niobate has not been synthesized, obtaining the other niobates is noteworthy on account of the fact that $CuNb_2O_6$ does not exhibit the perovskite structure, but is isostructural of the columbite (*13*). These polycrystalline powders are green in the case of tantalates and brown for niobates.

Electron Diffraction and High-Resolution Microscopy Study

No single crystal of these compounds could be obtained. An electron diffraction study was thus necessary. Several microcrystals of niobates $RbCu_3Nb_7O_{21}$ and $KCu_3Nb_7O_{21}$ were examined. From the electron diffraction diagrams (Fig. 1), it has been established that the cell of these oxides is orthorhombic with parameters close to those observed by Hussain and Kihlborg (*1*) for the ITB $K_{0.1}WO_3$ ($a \simeq 28$ Å, $b \simeq 7.5$ Å, $c \simeq 7.6$ Å). The indexation of the X-ray diffractograms confirms these results: the refined parameters obtained from these data (Table I) do not vary appreciably with the nature of A and M ions.

However, the reflection conditions—(hkl): $h + k = 2n$—involve the possible space groups $Cmm2$ and $Cmmm$ which are inconsistent with the model previously described for the HTB intergrowth (*1*).

An examination in high-resolution microscopy of these oxides confirms this difference with the ITB compounds $A_{0.1}WO_3$ (A = K, Rb). The high-resolution images of these phases exhibit rows of white spots distant from 14 Å, which can be assigned to the more voluminous hexagonal tunnels. Figure 2 shows, as an example, one of these

TABLE I

CELL PARAMETERS AND DENSITIES OF THE ORTHORHOMBIC $ACu_3M_7O_{21}$ OXIDES

A^+	M^V	$a \pm 0.01$ Å	$b \pm 0.004$ Å	$c \pm 0.005$ Å	$d_{obs} \pm 0.05$	d_{calc}
K	Nb	27.96	7.487	7.548	5.17	5.11_4
	Ta	28.06	7.505	7.531	7.70	7.67_7
Rb	Nb	28.08	7.519	7.579	5.30	5.24_2
	Ta	28.11	7.503	7.548	7.86	7.84_1
Cs	Nb	28.09	7.500	7.572	5.44	5.45_6
	Ta	28.15	7.502	7.538	8.17	8.03_9
Tl	Ta	28.04	7.500	7.515	8.45	8.39_8

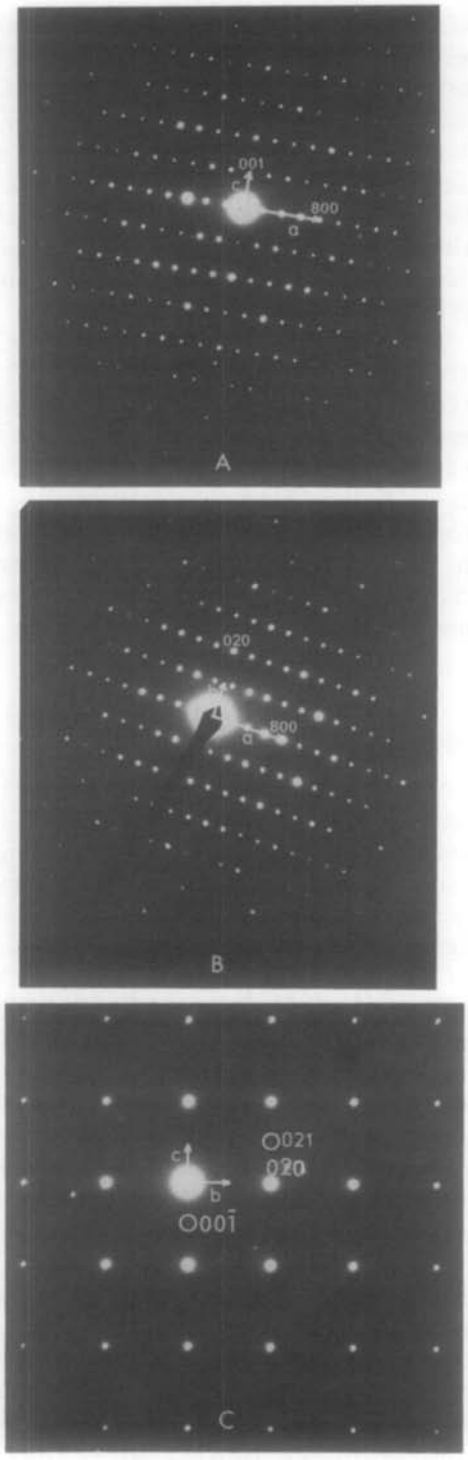

FIG. 1. Electron diffraction diagrams of $RbCu_3Nb_7O_{21}$: (a) hOl, (b) hkO, (c) Okl.

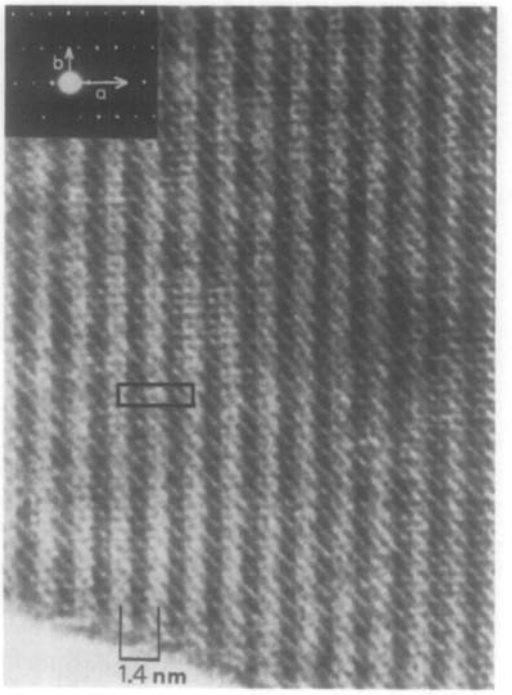

FIG. 2. High-resolution image of a $RbCu_3Nb_7O_{21}$ crystal. The electron beam is parallel to the c axis.

images observed for $RbCu_3Nb_7O_{21}$. This disposition of the hexagonal tunnels lets us think of a new type of intergrowth built up from single HTB rows separated by $CuTa_2O_6$ type slabs. (Fig. 3).

X-Ray Diffraction Study

In order to confirm this model, the structure of these compounds has been studied from the powder data. The measured densities (Table I) let four formular units $ACu_3M_7O_{21}$ appear which have been placed in the most symmetric space group *Cmmm* in order to have a minimum number of variable parameters.

Calculations were first made for $RbCu_3Ta_7O_{21}$: intensities of the first 50 reflections—i.e., 180 *hkl*—were measured. The atomic scattering factors used are those of Cromer and Waber (*14*) corrected for anomalous dispersion.

In a first step, the Rb, Ta, and O atoms

were placed according to the ideal model (Fig. 3) which corresponds to the single intergrowth HTB–ReO_3 type structure related to $K_{0.1}WO_3$. Although this model does not take into account the important tilting of the octahedra observed in $CaCu_3Ti_4O_{12}$, copper atoms have been distributed in an ordered manner over the nominal 12-fold perovskite sites. Three sites out of four have been filled with copper by analogy with this oxide. The temperature factors were fixed to an arbitrary value of 1 Å^2.

Refining the positions of the metallic heavy atoms lowered the discrepancy factor calculated on intensities to about 0.15. After refinement of the coordinates of copper and oxygen atoms and then of the *B* factors of all the atoms, the *R* factor reached a value close to 0.08. The atomic parameters corresponding to this refinement are given in Table II, except for oxygen atoms $O_{(8)}$ and $O_{(9)}$ which were located respectively in 4*f* ($\frac{1}{4}$ $\frac{1}{4}$ $\frac{1}{2}$) and 4*e* ($\frac{1}{4}$ $\frac{1}{4}$ 0) sites, while the Cu(4) site was empty and the Cu(2) site fully occupied.

At this stage of the resolution, an examination of the interatomic distances showed that they were all correct except for the Cu(2)–O distances which were too long. It appeared by comparison with the copper distorted perovskites that Cu(1) and Cu(3) had the same square coordination and that the corresponding sites could be fully occupied.

In order to obtain a correct square coordination for the remaining copper ions, the occupation by copper of the fourth perovskite site Cu(4) was considered. This distribution involved a splitting of the $O_{(8)}$ and $O_{(9)}$ oxygen atoms from 4*f* and 4*e* to 8*q* and 8*p* positions, respectively, with an occupancy factor of 0.5. These modifications did not significantly change the *R* factor which however was fixed to a lower value close to 0.06, for the final atomic parameters given in Table II.

Similar results were obtained for $RbCu_3Nb_7O_{21}$ (*R* = 0.07) and $TlCu_3Ta_7O_{21}$ (*R* = 0.09). However, in the latter case, the high thermal factor observed for Tl(*B* = 17 Å^2) led us to distribute this ion over two sorts of sites, 4*i* (o y o) and 8*p* (x y o) at about 0.5 Å from the tunnel axis in agreement with the results observed for the compound $Ca_2TlTa_5O_{15}$ which exhibits a related structure (*15*).

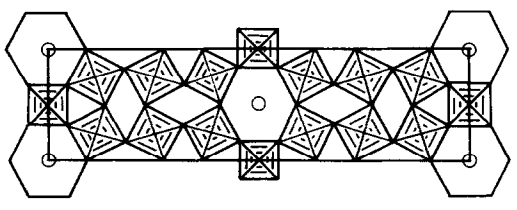

FIG. 3. Ideal model of the "M_7O_{21}" framework deduced from the electron microscopy observations.

Discussion

As shown from the projection of the structure on to the (0 0 1) plane (Fig. 4), the structural model predicted from the high-resolution microscopy study is confirmed by the X-ray investigation without any ambiguity.

Owing to the great number of variable parameters versus the limited number of data, the atomic coordinates cannot be considered as very accurate. Nevertheless, the interatomic distances obtained after refinement (Table III), close to those usually observed in ternary oxides, let us think that the distortions of the octahedral strings are significant.

The comparison of the structure with those of the intergrowth tungsten bronzes $A_{0.1}WO_3$ (*A* = K, Rb) (*1*), molybdenum antimony oxide $Sb_2Mo_{10}O_{31}$ (*16*), and tantalate $Ca_2TlTa_5O_{15}$ (*15*) shows that the host lattice of all these compounds can be formulated $|M_3O_9|^H_n\,|M_2O_6|^P_{n'}$ where $|M_3O_9|^H$ and $|M_2O_6|^P$ are respectively the narrowest

TABLE II

FINAL ATOMIC COORDINATES OF $RbCu_3Ta_7O_{21}$[a]

Atom	Position	x	y	z	B (Å)²
Rb(1)	2a	0	0	0	2.2(16)
Rb(2)	2d	0	0	0.5	2.5(16)
Cu(1)	4h	0.173(3)	0	0.5	2.2(12)
Cu(2) (τ = 0.5)	4h	0.321(7)	0	0.5	0.8(11)
Cu(3)	4g	0.318(8)	0	0	0.2(11)
Cu(4) (τ = 0.5)	4g	0.183(4)	0	0	2.3(21)
Ta(1)	4l	0.	0.5	0.244(7)	1.6(5)
Ta(2)	16r	0.1131(8)	0.2477(16)	0.255(3)	2.0(2)
Ta(3)	8m	0.25	0.25	0.252(5)	0.2(2)
O(1)	8o	0.088(4)	0	0.248(13)	1.7(23)
O(2)	8o	0.274(4)	0	0.220(15)	1.9(28)
O(3)	8o	0.366(4)	0	0.202(15)	2.4(31)
O(4)	16r	0.179(3)	0.164(5)	0.280(25)	0.6(21)
O(5)	16r	0.046(2)	0.304(8)	0.280(27)	0.8(24)
O(6)	8q	0.124(5)	0.322(12)	0.5	1.5(34)
O(7)	8p	0.128(5)	0.187(13)	0	2.7(33)
O(8) (τ = 0.5)	8q	0.236(9)	0.323(20)	0.5	2.4(36)
O(9) (τ = 0.5)	8p	0.238(9)	0.186(16)	0	2.4(34)
O(10)	2e	0.5	0	0.5	2.0
O(11)	2b	0.5	0	0	2.0

[a] The standard deviations are given in parentheses.

hexagonal tungsten bronze and perovskite slices which can be observed in the intergrowths. The host lattices of $Sb_2Mo_{10}O_{31}$ and $Ca_2TlTa_5O_{15}$ form thus the first term of this series ($n = n' = 1$) resulting from the intergrowth of single HTB–"M_3O_9" slices and single distorted perovskite "M_2O_6" slabs.

The framework "M_7O_{21}" (M = Nb, Ta) of our compounds corresponds to the intergrowth of single HTB "M_3O_9" slices (n = 1) where the A atoms are located (A = K, Rb, Cs, Tl) and double perovskite "M_4O_{12}" slabs ($n' = 2$) where copper ions are located while the $A_{0.1}WO_3$ bronzes (A = K, Rb) in spite of the similar size of their orthorhombic cell, exhibit an intergrowth

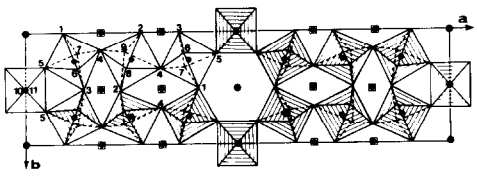

FIG. 4. Projection of the structure of $RbCu_3Ta_7O_{21}$ on to (001).

TABLE III

INTERATOMIC DISTANCES (Å) IN $RbCu_3Ta_7O_{21}$[a]

Ta-octahedron		Cu-polyhedron	
Ta(1)–O(5)	1.97(7) × 4	Cu(1)–O(4)	2.07(11) × 4
Ta(1)–O(11)	1.93(5) × 1	Cu(2)–O(6)	2.05(20) × 2
Ta(1)–O(10)	1.84(5) × 1	Cu(2)–O(8)	2.08(28) × 2
⟨Ta(1)–O⟩	1.94(6)	Cu(3)–O(2)	2.07(17) × 2
		Cu(3)–O(3)	2.04(19) × 2
Ta(2)–O(5)	1.95(4) × 1	Cu(4)–O(7)	2.09(16) × 2
Ta(2)–O(1)	1.99(4) × 1	Cu(4)–O(9)	2.08(24) × 2
Ta(2)–O(4)	1.96(8) × 1		
Ta(2)–O(3)	2.01(4) × 1	Rb-polyhedron	
Ta(2)–O(6)	1.95(4) × 1		
Ta(2)–O(7)	2.02(4) × 1	Rb(1)–O(1)	3.09(10) × 4
⟨Ta(2)–O⟩	1.98(4)	Rb(1)–O(5)	3.36(8) × 8
		Rb(1)–O(11)	3.751(4) × 2
Ta(3)–O(2)	2.01(4) × 2	Rb(1)–O(7)	3.86(14) × 4
Ta(3)–O(4)	2.11(8) × 2	Rb(2)–O(1)	3.11(10) × 4
Ta(3)–O(8)	1.98(7) × 1	Rb(2)–O(5)	3.10(8) × 8
Ta(3)–O(9)	1.99(9) × 1	Rb(2)–O(10)	3.751(4) × 2
⟨Ta(3)–O⟩	2.03(6)	Rb(2)–O(6)	4.24(12) × 4

[a] The standard deviations are given in parentheses.

built up from double HTB—"W_6O_{18}"—slabs and double perovskite "W_4O_{12}" slices.

Another particular feature of the $ACu_3M_7O_{21}$ compounds with respect to the other terms of the series concerns the different distortion of the strings, especially formed by the M(2)–O_6 and M(3)–O_6 octahedra along the ⟨010⟩ and ⟨001⟩ directions. This type of connection involves a drastic distortion of the 12-fold sites of the ideal perovskite, allowing a square coordination for copper.

Although the perovskite slabs exhibit deformations similar to those observed for $CaCu_3Ti_4O_{12}$, the remaining perovskite cages are too distorted to be occupied by calcium. However the great capability of calcium to accommodate various distorted sites, as shown for $Ca_2TlTa_5O_{15}$ (*15*), indicates that the possibility of formation of intergrowths containing both calcium and copper cannot be ruled out.

The results observed here show that the distortions introduced in the octahedral framework by the Jahn–Teller effect of copper favor the formation of HTB–perovskite intergrowths. Owing to its similar behavior, the introduction of trivalent manganese in these compounds should be considered.

References

1. A. Hussain and L. K. Kihlborg, *Acta Cryst.* A **32,** 551 (1976).
2. A. Hussain, *Chemica Scripta,* **11,** 224 (1977).
3. M. Marezio, P. D. Dernier, J. Chenavas, and J. C. Joubert, *J. Solid State Chem.* **6,** 16 (1973).
4. B. Bochu, J. Chenavas, J. C. Joubert, and M. Marezio, *J. Solid State Chem.* **11,** 88 (1974).
5. J. Chenavas, J. C. Joubert, M. Marezio, and B. Bochu, *J. Solid State Chem.* **14,** 25 (1975).
6. A. Deschanvres, B. Raveau, and F. Tollemer, *Bull. Soc. Chim. Fr.* **11,** 4077 (1967).
7. B. Bochu, M. N. Deschizeaux, J. C. Joubert, A. Collomb, J. Chenavas, and M. Marezio, *J. Solid State Chem.* **29,** 291 (1979).
8. V. Propach and D. Reinen, *Inorg. Nucl. Chem. Lett.* **7,** 569 (1971).
9. V. Propach, *Z. Anorg. Allg. Chem.* **435,** 161 (1977).
10. H. Vincent, B. Bochu, J. J. Aubert, J. C. Joubert, and M. Marezio, *J. Solid State Chem.* **24,** 245 (1978).
11. B. M. Gatehouse, *J. Less Common Metals* **50,** 139 (1976).
12. M. Ganne, R. Marchand, A. Verbaere, and M. Tournoux, *Mater. Res. Bull.* **13,** 109 (1978).
13. E. Husson, Y. Repelin, Nguyen Quy Dao, and H. Brusset, *Mater. Res. Bull.* **12,** 1199 (1977).
14. D. T. Cromer and J. T. Waber, *Acta Crystallogr.* **12,** 104 (1965).
15. M. Ganne, M. Dion, A. Verbaere, and M. Tournoux, *J. Solid State Chem.* **29,** 9 (1979).
16. M. Parmentier, C. Gleitzer, A. Courtois, and J. Protas, *Acta Crystallogr. B* **35,** 1963 (1979).